

# Impact of Chromium Oxide Nanoparticles on Growth and Biofilm Formation of Persistence *Klebsiella pneumoniae* Isolates

Mohammed Al Marjani<sup>1</sup>, Sarah Naji Aziz<sup>1</sup>, Ahmed Mahdi Rheima<sup>2</sup>, Zainab Sabri Abbas<sup>1</sup>

<sup>1</sup>Department of Biology, College of Science, Mustansiriyah University, Baghdad, Iraq.

<sup>2</sup>Department of Chemistry, College of Science, Wasit University, Kut, Iraq.

✉ Corresponding author. E-mail: arahema@uowasit.edu.iq

**Received:** Dec. 11, 2020; **Accepted:** Aug. 5, 2021; **Published:** Sep. 10, 2021

**Citation:** Mohammed Al Marjani, Sarah Naji Aziz, Ahmed Mahdi Rheima, and Zainab Sabri Abbas, Impact of Chromium Oxide Nanoparticles on Growth and Biofilm Formation of Persistence *Klebsiella pneumoniae* Isolates. *Nano Biomed. Eng.*, 2021, 13(3): 321-327.

**DOI:** 10.5101/nbe.v13i3.p321-327.

## Abstract

Bacterial persistence is recognized as a major cause of antibiotic therapy failure, causing biofilms and chronic intractable infections. The emergence of persisters in *K. pneumoniae* isolates has become a worldwide public health concern. Despite this clinical threat, currently, there are no viable means for eradicating *K. pneumoniae* persisters. In this project, chromium oxide ( $\text{Cr}_2\text{O}_3$ ) nanoparticles were synthesized by the photochemical method. The morphology, topographic and physical properties of nano-synthesized were described by transmission electron microscopy (TEM), atomic force microscopy (AFM), X-ray powder diffraction (XRD), and ultraviolet-visible spectroscopy (UV. vis) measurements. The obtained average size of  $\text{Cr}_2\text{O}_3$ -NPs was to be ranging from 11 to 30 nm. The activities of the  $\text{Cr}_2\text{O}_3$ -NPs for antibacterial and antibiofilm formation against persistent *K. pneumoniae* were assessed. The result showed a significant inhibitory effect of  $\text{Cr}_2\text{O}_3$ -NPs against *K. pneumoniae*. A, where the zones of inhibition were 12-18 mm, and the minimum inhibitory concentration (MIC) was 625  $\mu\text{g}/\text{mL}$ . The concentration of  $\text{Cr}_2\text{O}_3$ -NPs of 10 mg/mL demonstrated the highest inhibition activity against biofilm formation ( $73.95 \pm 2.17\%$ ), indicating the lowest inhibition ( $19.08 \pm 1.32\%$ ) at a level of 0.625 mg/mL.  $\text{Cr}_2\text{O}_3$ -NPs therefore had a positive impact on biofilms that were produced by persistence isolates of *K. pneumoniae*.

**Keywords:**  $\text{Cr}_2\text{O}_3$ -NPs, Photochemical method, Persistence *Klebsiella pneumoniae*, Antibacterial, Antibiofilm

## Introduction

*Klebsiella pneumoniae* (*K. pneumoniae*), belonging to the Enterobacteriaceae family, is a gram-negative, non-motile, encapsulated, and opportunistic bacterium which often populates the mouth, skin, gastrointestinal and respiratory tracts, and it is also utilized in medical devices [1]. *K. pneumoniae* is an important pathogen, which causes hospital-acquired severe infections such as the most common hospital-acquired pneumonia

(HAP) [2]. Community-acquired and a wide range of nosocomial infections including urinary tract infections, pneumonia, pyogenic liver abscesses, endogenous endophthalmitis, and septicaemia. Currently, with the recent emergence and widespread of hypervirulent and antibiotics resistant strains, *K. pneumoniae* has gained notoriety as an infectious agent due to a rise in the number of severe infections and the increasing lack of effective treatments as such, it has become a significant health concern [3].

Antibiotic therapy failure is known as a global seizure that is typically attributed to resistance. Studies have opened up many genetic resistance mechanisms that caused a respectable decrease in the effective concentration of antibiotics [4]. It has also been realized that persistence formation in the bacterial population makes a small subpopulation of bacterial cells survive under high concentrations of antibiotic exposure [5].

One of the major causes of antibiotic therapy failure is bacterial persistence which is recognized as causing chronic intractable infections. Persisters are defined as a subpopulation of susceptible bacteria that survive when a bacterial culture is exposed to lethal doses of bactericidal antibiotics. Different from drug-resistant mutants with genetic modification, persisters do not replicate and constitute a minority of antimicrobial tolerant cells without a heritable resistance mechanism [6, 7]. Persister cells are genetically identical to antibiotic susceptible cells within a population that does not rely on (MIC) values, bacterial persistence but have a distinct phenotype in that they are survivable by antibiotics at concentrations that would further, be fatal [8]. Persister cells are displayed to pre-exist in the bacterial populations before the addition of the antibiotic, being dormant or slow-growing by phenotypic switching [9]. After antibiotics are removed, the surviving persisters reback to grow in a new heterogeneous population with sensitive and tolerant subpopulations, in the same way as the whole original culture [8].

In general, the nanomaterials are known for considerable microbicidal activity rather than conventional antibiotics and even showed responses against different types of cells [10].

The metal nanoparticles, such as Cr, Ag, Au, and Pt NPs, are considered a great interest source because of the unique and novel electrical, optical, physical, chemical, and magnetic proprieties [11-13]. These metal nanoparticles have been used in cosmetics, sensors, biomedicine, pathogen detection, diagnostics, antigen detection, enzymes, vaccines, and radiology. Among the various transition metal oxide-based NPs, chromium oxide ( $\text{Cr}_2\text{O}_3$ ) has attracted special attention due to its high stability, high melting temperature. Chromium (Cr) is a transitional metal that can exist in different oxidation states.  $\text{Cr}^{3+}$  is an essential nutrient necessary for the normal metabolism of carbohydrates; the deficiency of  $\text{Cr}^{3+}$  leading to glucose intolerance [14].  $\text{Cr}^{3+}$  complexes with

different ligands were shown to have antimicrobial activity. Therefore, the present study aims to Synthesis of chromium oxide ( $\text{Cr}_2\text{O}_3$ ) nanoparticles and to investigate the antibacterial and antibiofilm effects of  $\text{Cr}_2\text{O}_3$ -NPs on persistence *K. pneumoniae* isolates.

## Experimental

### Bacterial isolates and growth conditions

*Klebsiella pneumoniae* isolates from clinical sources were obtained from different hospitals in Baghdad. All isolates were identified using the Vitek-2 system. All bacterial isolates were grown on Luria-Bertani (LB, Difco Laboratories) agar plates or in LB broth at 37 °C.

### Detection of persister cells

Persister cells assay was determined by rapidly killing normal growing cells using a combination of lytic solutions [15]. Briefly, *K. pneumoniae* isolates were grown overnight in LB broth at 37 °C and then diluted to equal to 0.5 McFarland standard. 1 mL was taken from 0.5 McFarland and 200  $\mu\text{L}$  of the lysis solution was added in a 10 mL test tube and mixed with vortex for 10 seconds and incubated at room temperature for 10 min. After that, 200  $\mu\text{L}$  of the enzymatic lysis solution was added to the mixture and gently mixed. Finally, incubated at 37 °C for 15 min at 200 rpm. 10  $\mu\text{L}$  spread on LB plates for measuring the frequencies of persister cells.

### Biofilm assay

The evaluation of *K. pneumoniae* biofilm Formation ability was carried out as the protocol described by Badmasti et al. [16]. First, *K. pneumoniae* were inoculated in brain heart infusion (BHI) broth + 2% (w/w) glucose overnight. Then the growth was diluted to 1:100 in fresh BHI broth medium, and 100  $\mu\text{L}$  of diluted culture was pipetted into the wells of 96-well polystyrene plate and incubated for 24 h at 37 °C. After incubation, the plates were washed with sterile phosphate-buffered saline (PBS) three times and left to air dry at room temperature before being stained with 200  $\mu\text{L}$  of crystal violet 1% for 15 min. After drying at room temperature, the stain was eluted with 200  $\mu\text{L}$  of 95% of ethanol and the optical density was quantified at 570 nm using an ELISA reader. The assay was carried out in triplicate. The adherence capacities of the assay isolates were classified into four categories; the mean optical density of the negative control was

counted as:

$OD \leq OD_c$ , the bacteria were non-adherent;

If  $OD_c < OD \leq 2 \times OD_c$ , the bacteria were weakly adherent;

If  $2 \times OD_c < OD \leq 4 \times OD_c$ , the bacteria were moderately adherent;

If  $4 \times OD_c < OD$ , the bacteria were strongly adherent.

### Synthesis of chromium oxide ( $Cr_2O_3$ ) nanoparticles

The photolysis process [17, 18] has been used to fabricate chromium oxide ( $Cr_2O_3$ ) nanoparticles. The photocell contains a 125 W UV mercury lamp with a wavelength of 365 nm and an ice bath-cooled pyrex tube that prevented an increase in temperature due to UV radiation. Accordingly, 0.5 g of chromium nitrate  $Cr(NO_3)_3$  was dissolving in a 50 mL de-ionized water; then, 50 mL, 1 M of urea was added slowly (drop by drop) to the solution with stirred for 2 h. The solution was irradiated for 30 min, and a brown precipitate was presented. The precipitation was isolated and washed several times using a centrifuge with de-ionized water. After drying the material for one day and calcinating it in an oven at 500 °C for 3 h, a black-green precipitate chromium oxide nanoparticles were produced.

### Characterization of chromium oxide nanoparticles

The powdered specimen was placed on a glass slide, and XRD of  $Cr_2O_3$ -NPs was examined using (XRD-6000), it is achieved at 30 mA and 40 kV to generate radiation at a wavelength of 1.5406 Å. TEM measurement type JEOL JEM-2100 was used to study the size and morphology of nanoparticles. A drop of suspended nanoparticles was placed on the carbon-coated TEM grid for analysis. Atomic force microscope is known as AFM-related specification (AA 3000 sample microscope) to measure the surface of the  $Cr_2O_3$ -NPs.

### Antibacterial activity and MIC of $Cr_2O_3$ -NPs

Antibacterial activity of  $Cr_2O_3$ -NPs against persistence *K. pneumoniae* isolates was tested using the agar well diffusion method [19]. The minimum inhibitory concentration was employed by using the 96-well microtiter plate. Briefly, 100 µL of LB broth was added to microtiter plate wells, then wells of the first vertical row (A1-A10) were filled with 100 µL of  $Cr_2O_3$ -NPs (10 mg/mL) followed by mixing

1:2 serial dilutions. 100 µL from the last well was discarded. Finally, all wells (except negative control row A11-H11, which filled only with LB broth) were filled with 5 µL of *K. pneumoniae* bacterial diluted suspension ( $10^8$  CFU/mL or  $10^5$  CFU/well) after 24 h of incubation, 10 µL of resazurin dye was added to the wells and incubated for 4 h at 37 °C to be ready for reading, the actions of different concentrations of  $Cr_2O_3$ -NPs for the bacterial growth were detected by using UV visible spectrophotometer.

### Antibiofilm effect of $Cr_2O_3$ -NPs

The antibiofilm effect of  $Cr_2O_3$ -NPs on persistence *K. pneumoniae* isolates was tested as previously described by [21]. Briefly, *K. pneumoniae* isolates were inoculated in BHI broth at 37 °C. The next day, the growing culture was diluted to  $OD_{595} = 0.137$ . After that, 20 µL of bacterial dilution was inoculated in the wells of microtiter plates containing 80 µL of BHI broth with 2% sucrose, and 100 µL of  $Cr_2O_3$ -NPs were added and mixed well then incubated for 24 h at 37 °C. After two washes with PBS for evacuating the wells, the plate left to be dried at room temperature. Unattached bacterial cells were removed. 200 µL of 0.1% crystal violet solution was used for biofilm staining. The stain was eluted with 200 µL of pure ethanol and the optical density was quantified at 630 nm using an ELISA reader. The negative control was filled with LB broth only, while the biofilm production with bacterial suspension without  $Cr_2O_3$ -NPs were positive controls. The assay was carried out in triplicate. To calculate the rate of inhibition caused by  $Cr_2O_3$ -NPs, the following formula was used

$$\text{Inhibition rate (\%)} = \frac{(\text{Control OD} - \text{Treated OD})}{(\text{Control OD})} \times 100$$

### Statistical analysis

The data results of this study were analyzed by using Graph Pad Prism 8 software and Microsoft Excel 2013 for each biological replicate. The level of probability at P-value  $\leq 0.05$  that used to identify a significant difference.

## Results and Discussion

### Detection of persister cells formation

*Klebsiella pneumoniae* isolates were tested for phenotypic detection of persister cell formations by using a rapidly killing method. Results show that out of 30 *K. pneumoniae* isolates, 5/30 isolates were persister cells formation as shows in Fig. 1. This

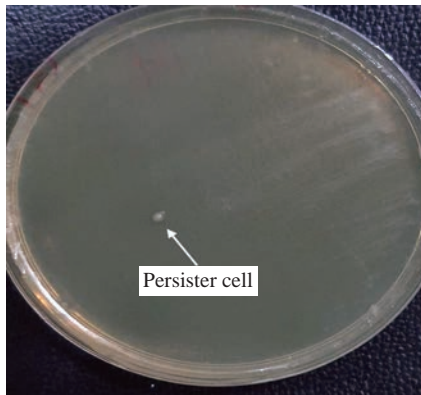


**Fig. 1** Persister cells formations in *K. pneumoniae* by rapidly killing method.

method of persister cell isolation is significantly faster than traditional methods that depend on antibiotic concentrations. Additionally, the rapidly killing process is stably maintained after isolation to allow more studies on the isolated persister cells. So it is an optimal protocol that carries out without any effect on the bacterial population size, the bacterial strain, and the cultural physiological state.

### Cr<sub>2</sub>O<sub>3</sub>-NPs synthesis and characterization

The XRD of Cr<sub>2</sub>O<sub>3</sub>-NPs photochemically synthesized as shown in Fig. 2. The peak of Cr<sub>2</sub>O<sub>3</sub> is

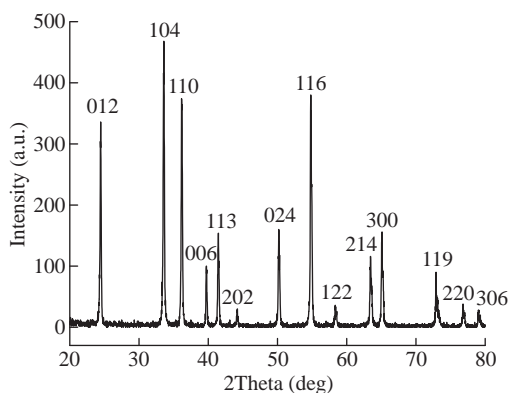


**Fig. 2** XRD pattern of the Cr<sub>2</sub>O<sub>3</sub>-NPs.

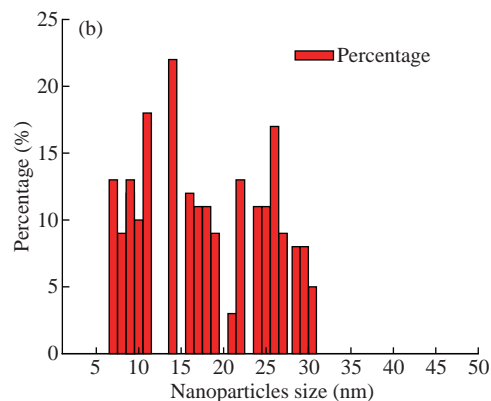
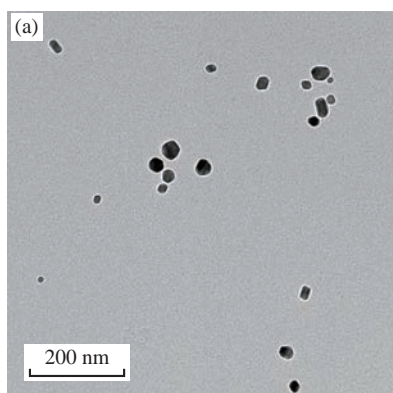


**Fig. 3** (a) TEM image of synthesized Cr<sub>2</sub>O<sub>3</sub>-NPs; (b) TEM nanoparticles distribution.

shown to be highly pure, and peaks are not observed for other materials. It shows sharp peaks suggesting high nanoparticles of crystalline type. The XRD pattern of Cr<sub>2</sub>O<sub>3</sub>-NPs showed a particular peak of diffraction 24.4°, 33.5°, 36.1°, 39.7°, 41.4°, 44.1°, 50.2°, 54.8°, 57.1°, 58.3°, 63.4°, 65.1°, 73.3°, 76.8° and 79° at 2θ values indexed to 012, 104, 110, 006, 113, 202, 024, 116, 211, 122, 214, 300, 119, 220 and, 306 were due to the crystal structure of Cr<sub>2</sub>O<sub>3</sub> [JCPDS No. 00-038-1479]. According to the Debye-Scherrer formula (plane 104), the average crystallite size was determined to be 12.65 nm [18, 22].

The general morphology of as-grown Cr<sub>2</sub>O<sub>3</sub>-NPs was determined by a transmitting electron microscopy (TEM) technique. Fig. 3 shows an as-grown material typical image. The figure shows that the majority of nano sizes are spherical shape. The image demonstrates that Cr<sub>2</sub>O<sub>3</sub>-NPs furthermore without any aggregation. The zero dimension and formation particles have been proven in the measurement of a transmission electron microscope, as all the dimensions of the formed particle are less than 100 nanometers, It is free from any clusters and the reason is due to the photosynthetic method, which gives small particles and is devoid of any clusters. The average size of the nanoparticles is a range between 11 to 30 nm.

An atomic force microscope (AFM) was used to determine the average particle size of synthesized Cr<sub>2</sub>O<sub>3</sub>-NPs, as shown in Fig. 4. All the nanoparticles have a crystal configuration. Particles are equally distributed across a range of 3D images within the scanning region (Fig. 4(a)). This surface can be classified as a necessity in medical applications. Fig. 4(b) shows the gaussian distribution of nanoparticles, as it shows the particle mean of Cr<sub>2</sub>O<sub>3</sub>-NPs was 17.62 nm. The particle 7 nm was the smaller diameter obtained. This result has been confirmed by TEM.

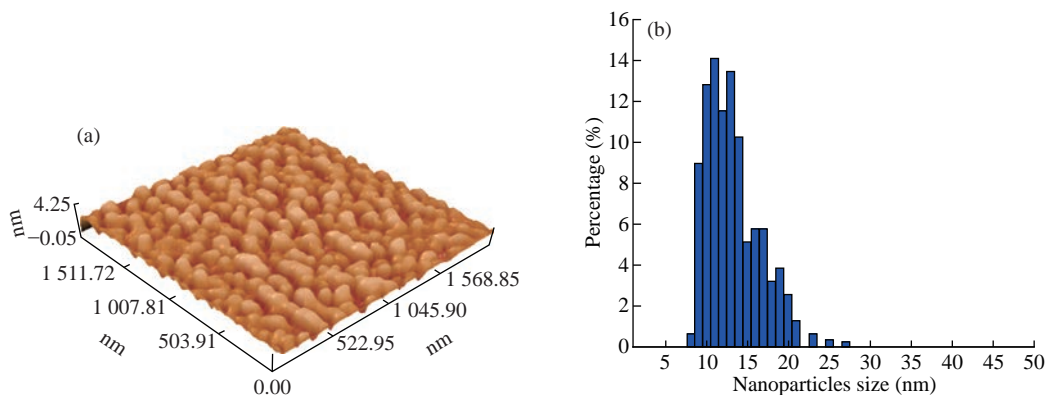


Fig. 4 (a) AFM image of 3D surface of the Cr<sub>2</sub>O<sub>3</sub> nano-synthesized; (b) Distribution of Cr<sub>2</sub>O<sub>3</sub>-NPs from AFM.

### Antibacterial activity and MIC of Cr<sub>2</sub>O<sub>3</sub>-NPs

The antibacterial efficacies of Cr<sub>2</sub>O<sub>3</sub>-NPs were detected on persistence *K. pneumoniae*. Cr<sub>2</sub>O<sub>3</sub>-NPs showed considerable antibacterial activity in the agar well diffusion method, as the inhibition zones were 18 and 12 mm in values of 10.000 and 1000 µg/mL, respectively (Fig. 5). The MIC demonstrates that Cr<sub>2</sub>O<sub>3</sub>-NPs had a high-achievement antibacterial at 625 µg/mL. Moreover, the growth ability of persistence *K. pneumoniae* was frequently reduced during 14 h of Cr<sub>2</sub>O<sub>3</sub>-NPs exposure.

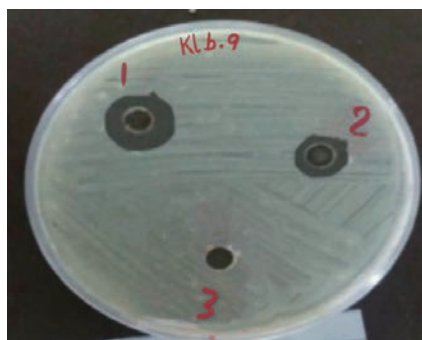


Fig. 5 Antibacterial activity in the agar-well diffusion method showing inhibition zone of Cr<sub>2</sub>O<sub>3</sub>-NPs against *K. pneumoniae* filled with 10.000 µg/mL in well 1 and 10.000 µg/mL in well 2, while well 3 filled with D.W as a control.

### Biofilm inhibition activity

In this study, the investigation of Cr<sub>2</sub>O<sub>3</sub>-NPs to inhibit the biofilm produced by persister cells of *K. pneumoniae* isolates was done. The average inhibition rate of Cr<sub>2</sub>O<sub>3</sub>-NPs toward *K. pneumoniae* was elaborated. The biofilm inhibition was carried out significantly by Cr<sub>2</sub>O<sub>3</sub>-NPs. The inhibition of biofilm was 73.95±2.17% and 19.08±1.32% in values of 10 mg/mL and 0.625 mg/mL, respectively. Thus, Cr<sub>2</sub>O<sub>3</sub>-NPs showed a considerable effect on biofilms formed by persister cells of *K. pneumoniae* isolates.

### Discussion

*Klebsiella pneumoniae* is an urgent bacteria causing a wide gauge of community and hospital-acquired infections. During the last contract, the prevalence of multidrug-tolerant *K. pneumoniae* isolates has become a worldwide public health concern [3]. Bacterial persistence represents a small subpopulation of bacteria that survives killing with lethal concentrations of bactericidal antibiotics [24-26]. Persistence is the intermediate stage between sensitive wild strain and resistant mutant before resistance is established. Bacterial persistence is recognized as a major cause of

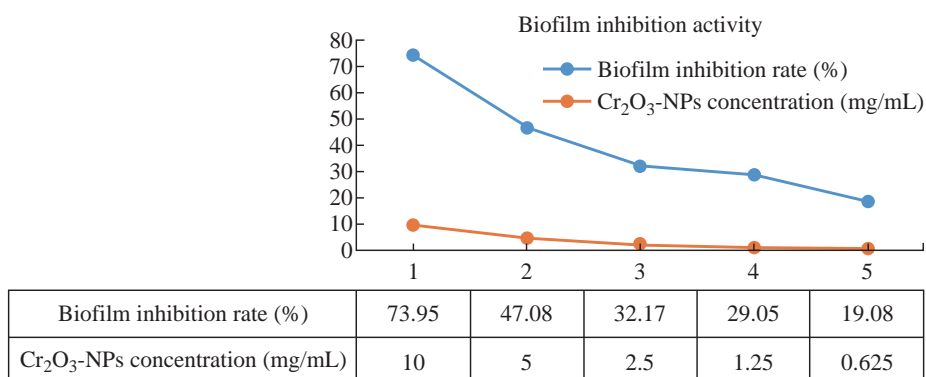


Fig. 6 Biofilm inhibition activity of Cr<sub>2</sub>O<sub>3</sub>-NPs against clinical isolates of persistence *K. pneumoniae*.

antibiotic therapy failure, causing chronic intractable infections [27].

If we are capable of inhibiting persistence, bacterial resistance to antibiotics and drugs would decrease and help in improving chronic infections. Here, we investigated the presence of persister cells in the *K. pneumoniae* isolates after tested with alkaline and enzymatic lysis solutions by using a rapidly killing method. We also investigated the effect of Cr<sub>2</sub>O<sub>3</sub>-NPs on *K. pneumoniae* persister cells as an antibacterial and antibiofilm formation agent. According to several reports [28, 29], Cr<sub>2</sub>O<sub>3</sub>-NPs improved the antimicrobial activity toward a wide range of microbial pathogens. In the current study, we found that the Cr<sub>2</sub>O<sub>3</sub>-NPs treatments would be one of the most effective antibacterial agents ( $p < 0.05$ ) as the inhibition zones were 18 and 12 mm in values of 10.000 and 1000 µg/mL, respectively to eradicate *K. pneumoniae* persister cells. The MIC of Cr<sub>2</sub>O<sub>3</sub>-NPs, for *K. pneumoniae* isolates, was 625 µg/mL. Results emphasized that Cr<sub>2</sub>O<sub>3</sub>-NPs showed significant activity to inhibit biofilm formation by *K. pneumoniae* persister cells (19.08±1.32%, 28.04±0.88%, 34.83±1.34%, 47.04±1.39%, and 73.95±2.17%) with values of 0.625, 1.25, 2.5, 5 and 10 mg/mL respectively. Ranjani et al. [30] showed that the green nano colloid (ApNc) had potent antibacterial and antibiofilm activity against antibiotic-resistant strains isolated from tannery effluent, and in another study Ranjani et al. [31] recorded that Endophytic fungal silver nanoparticles (Ag NPs) could be the potential alternative to antibiotics to treat the infections caused by *P. aeruginosa*.

## Conclusions

To improve bactericidal activity, Cr<sub>2</sub>O<sub>3</sub>-NPs were successfully synthesized by a photolysis method. The synthesized Cr<sub>2</sub>O<sub>3</sub>-NPs showed a spherule shape with an average size of the nanoparticles in a range between 11 to 30 nm as calculated randomly from TEM. AFM and TEM study unveiled the crystal nature of the nanoparticles without any agglomeration. The effective role of the Cr<sub>2</sub>O<sub>3</sub>-NPs against bacterial growth and biofilm formation was assessed against persistence *K. pneumoniae*. Overall, the current study was the first to have shown that Cr<sub>2</sub>O<sub>3</sub>-NPs are effective in inhibiting biofilm formation of *K. pneumoniae* persister cells in vitro.

## Conflict of Interests

The authors declare that no competing interest exists.

## References

- [1] Q. Peng M. Fang X. Liu et al., Isolation and characterization of a novel phage for controlling multidrug-resistant *Klebsiella pneumoniae*. *Microorganisms*, 2020, 8(4): 542.
- [2] Y. Zuo, D. Zhao, G. Song, et al., Risk Factors, Molecular Epidemiology, and Outcomes of Carbapenem-Resistant *Klebsiella pneumoniae* Infection for Hospital-Acquired Pneumonia: A Matched Case-Control Study in Eastern China During 2015-2017. *Microbial Drug Resistance*, 2020.
- [3] N. Narimisa, F. Amraei, B.S. Kalani, et al., Effects of sub-inhibitory concentrations of antibiotics and oxidative stress on the expression of type II toxin-antitoxin system genes in *Klebsiella pneumoniae*. *Journal of Global Antimicrobial Resistance*, 2020, 21: 51-56.
- [4] X. Zhang, S. Yan, J. Chen, et al., Physical, chemical, and biological impact (hazard) of hospital wastewater on environment: the presence of pharmaceuticals, pathogens, and antibiotic-resistance genes. *Current Developments in Biotechnology and Bioengineering*. Elsevier, 2020: 79-102.
- [5] Y. Li, L. Zhang, Y. Zhou, et al., Survival of bactericidal antibiotic treatment by tolerant persister cells of *Klebsiella pneumoniae*. *Journal of Medical Microbiology*, 2018, 67(3): 273-281.
- [6] G.M. Knudsen, Y. Ng, and L. Gram, Survival of bactericidal antibiotic treatment by a persister subpopulation of *Listeria monocytogenes*. *Appl Environ Microbiol*, 2013, 79: 7390-7397.
- [7] B. Van den Bergh, M. Fauvart, and J. Michiels, Formation, physiology, ecology, evolution and clinical importance of bacterial persisters. *FEMS Microbiol Rev*, 2017, 41: 219-251.
- [8] S.H. Jung, C.M. Ryu, and J.S. Kim, Bacterial persistence: Fundamentals and clinical importance. *Journal of Microbiology*, 2019, 57(10): 829-835.
- [9] N.Q. Balaban, J. Merrin, R. Chait, et al., Bacterial persistence as a phenotypic switch. *Science*, 2004, 305: 1622-1625.
- [10] A.M.B. Sadiq, I. Ali, N. Muhammad, et al., Synthesis and antimicrobial activity of zinc oxide nanoparticles against foodborne pathogens *Salmonella typhimurium* and *Staphylococcus aureus*. *Biocatalysis and Agricultural Biotechnology*, 2019, 17: 36-42.
- [11] J. Jeevanandam, A. Barhoum, Y.S. Chan, et al., Review on nanoparticles and nanostructured materials: history, sources, toxicity, and regulations. *Beilstein Journal of Nanotechnology*, 2018, 9(1): 1050-1074.
- [12] J.L. Elechiguerra, Interaction of silver nanoparticles with HIV-1. *Journal of Nanobiotechnology*, 2005, 3(1): 6.
- [13] A.R. Siekkinen, Rapid synthesis of small silver nanocubes by mediating polyol reduction with a trace amount of sodium sulfide or sodium hydrosulfide. *Chemical Physics Letters*, 2006, 432(4-6): 491-496.
- [14] M.A. Mohammed, A.M. Rheima, S.H. Jaber, et al., The removal of zinc ions from their aqueous solutions by Cr<sub>2</sub>O<sub>3</sub> nanoparticles synthesized via the UV-irradiation method. *Egyptian Journal of Chemistry*, 2020, 63(2): 425-431.
- [15] S.J. Cañas-Duarte, S. Restrepo, and J.M. Pedraza, Novel

- protocol for persister cells isolation. *PLoS One*, 2014, 9(2): e88660.
- [16] F. Badmasti, S.D. Siadat, S. Bouzari, et al., Molecular detection of genes related to biofilm formation in multidrug-resistant *Acinetobacter baumannii* isolated from clinical settings. *Journal of Medical Microbiology*, 2015, 64(5): 559-564
- [17] A.M. Rheima, M.A. Mohammed, S.H. Jaber, et al., Synthesis of silver nanoparticles using the UV-irradiation technique in an antibacterial application. *Journal of Southwest Jiaotong University*, 2019, 54(5).
- [18] D.H. Hussain, A.M. Rheima, S.H. Jaber, et al., Cadmium ions pollution treatments in aqueous solution using electrochemically synthesized gamma aluminum oxide nanoparticles with DFT study. *Egyptian Journal of Chemistry*, 2020, 63(2): 417-424.
- [19] S.M. Yaseen, H.A. Abid, A.A. Kadhim, Et al., Antibacterial activity of palm heart extracts collected from Iraqi *Phoenix dactylifera L.* *Journal of Techniques*, 2019, 1(1): 52-59.
- [20] C.H. Teh, W.A. Nazni, A. Norazah, et al., Determination of antibacterial activity and minimum inhibitory concentration of larval extract of fly via resazurin-based turbidometric assay. *BMC Microbiology*, 2017, 17(1): 36.
- [21] N.A. Theodora, V. Dominika, and D.E. Waturangi, Screening and quantification of anti-quorum sensing and antibiofilm activities of phyllosphere bacteria against biofilm-forming bacteria. *BMC Research Notes*, 2019, 12(1): 732.
- [22] A.M. Rheima, M.A. Mohammed, S.H. Jaber, et al., Adsorption of selenium ( $\text{Se}^{4+}$ ) ions pollution by pure rutile titanium dioxide nanosheets electrochemically synthesized. *Desalination and Water Treatment*, 2020, 194: 187-193.
- [23] Ö.B. Mergen, E. Arda. Determination of Optical Band Gap Energies of CS/MWCNT Bio-nanocomposites by Tauc and ASF Methods. *Synthetic Metals*, 2020, 269: 116539.
- [24] R. Singh, P. Ray, A. Das, et al., Role of persisters and small-colony variants in antibiotic resistance of planktonic and biofilm-associated *Staphylococcus aureus*: an in vitro study. *J. Med. Microbiol.*, 2009, 58: 1067-1073.
- [25] N. Möker, C.R. Dean, and J. Tao, *Pseudomonas aeruginosa* increases the formation of multidrug-tolerant persister cells in response to quorum-sensing signaling molecules. *Journal of Bacteriology*, 2010, 192(7): 1946-1955.
- [26] V. Leung, C.M. Lévesque, A stress-inducible quorum-sensing peptide mediates the formation of persister cells with noninherited multidrug tolerance. *Journal of bacteriology*. 2012, 194(9): 2265-2274.
- [27] R.A. Fisher, B. Gollan, and S. Helaine, Persistent bacterial infections and persister cells. *Nature Reviews Microbiology*, 2017, 15(8): 453.
- [28] P.R. Nivethitha, D.C. Rachel, A study of antioxidant and antibacterial activity using honey mediated Chromium oxide nanoparticles and its characterization. *Materials Today: Proceedings*, 2020.
- [29] M.A. Subhan, S.S. Jhuma, P.C. Saha, et al., Efficient selective 4-aminophenol sensing and antibacterial activity of ternary  $\text{Ag}_2\text{O}_3 \cdot \text{SnO}_2 \cdot \text{Cr}_2\text{O}_3$  nanoparticles. *New Journal of Chemistry*, 2019, 43(26): 10352-10365.
- [30] S. Ranjani, B.I. Faridha, I.K. Tasneem, et al., Silver decorated green nano colloids as a potent antibacterial and antibiofilm agent against antibiotic-resistant organisms isolated from tannery effluent. *Inorganic, and Nano-Metal Chemistry*, 2020.
- [31] S. Ranjani, A.M. Shariq, M. Adnan, et al., Synthesis, characterization, and applications of endophytic fungal nanoparticles. *Inorganic and Nano-Metal Chemistry*, 2021, 51(2): 280-287.

**Copyright**© Mohammed Al Marjani, Sarah Naji Aziz, Ahmed Mahdi Rheima, and Zainab Sabri Abbas. This is an open-access article distributed under the terms of the Creative Commons Attribution License, which permits unrestricted use, distribution, and reproduction in any medium, provided the original author and source are credited.